# A Simple ICI Suppression Method Utilizing Cyclic Prefix for OFDM Systems in the Presence of Phase Noise

Chun-Ying Ma, *Student Member, IEEE,* Chun-Yen Wu, and Chia-Chi Huang

***Abstract*—An extremely low-complexity inter-carrier interference (ICI) suppression method for OFDM systems in the presence of phase noise is proposed in this paper. The core idea is to utilize the ISI-free part of cyclic prefix (CP), which is simply ignored in traditional methods. We linearly combine the ISI-free samples in CP with the corresponding samples in the OFDM symbol to suppress ICI, and this scheme is called '*CP combining*' throughout this paper. In addition, the optimum combining coefficients, in the sense of ICI power minimization, are derived, and a set of near-optimum coefficients are proposed to reduce the complexity. Simulation results show that the proposed CP combining method improves the system performance by $0.5-1.5$dB. Furthermore, the proposed method can be incorporated with other phase noise mitigation methods to further improve the system performance.**

***Index Terms*—Phase noise, ICI suppression, CP combining, low-complexity, windowing, 60GHz.**

## I. Introduction

ORTHOGONAL Frequency Division Multiplexing (OFDM) is the key modulation technique widely used in modern and next-generation wireless communication systems, such as WiMAX, LTE-Advanced, and wireless local area networks, mainly for three reasons. First, it can effectively combat the inter-symbol interference (ISI) caused by a multipath channel by dividing a wideband frequency-selective channel into many narrowband frequency-flat subchannels. Second, the receiver is simple since it requires only one Fast Fourier Transform (FFT) chip and a one-tap equalizer. Last but not least, power and bit loading algorithms can be employed to further increase the power and spectral efficiency.

However, phase noise, which is caused by the imperfection of the local oscillator, is detrimental to OFDM systems. Phase noise causes not only common phase error (CPE), which rotates the received signal, but also inter-carrier interference (ICI), which destroys the orthogonality among subcarriers. The effect of phase noise has been analyzed in [1]–[7], and it is shown from these works that phase noise is a critical issue on system performance. Consequently, many phase noise mitigation methods have been proposed in literature e.g., [8]–[22]. In [8], [9], simple methods for CPE estimation and phase noise suppression were proposed. The authors in [10] proposed a low-complexity ICI mitigation method by dividing the entire OFDM symbol into a number of subblocks. In [11]–[14], [17], [18], joint estimation algorithms for channel impulse response, frequency offset, and phase noise were proposed. In [12], the authors reduced the complexity of ICI mitigation algorithms by treating the time-domain phase noise as static within $K$ samples. In [13]–[16], the authors reduced the overall complexity by interpolating the time-domain phase noise process. Through approximating phase noise by a band-limited process, Petrovic *at el.* proposed a method to reduce the complexity of phase noise parameter estimation in [19]. In [20], the phase noise process was modeled as a power series to reduce the complexity in parameter estimation. A low-complexity method incorporating error correcting codes and adaptive algorithms to track phase noise was proposed in [21]. Finally, a blind compensation method was proposed in [22]. However, since it only works for constant modulus modulation, this method is limited in its applications.

In this paper, we concentrate on a different scheme: the cyclic prefix (CP) *recycling* scheme. The CP recycling scheme is motivated by the fact that in some situations the specified CP length is much longer than the delay spread and there are a considerable number of ISI-free samples in CP. Conventionally, these ISI-free samples are simply discarded, and apparently it is a waste of resources. Therefore, the core idea of this scheme is to design a method to *recycle* the ISI-free samples in CP to improve the system performance. Originally, the CP recycling scheme was used to maximize signal-to-noise ratio (SNR) in the presence of frequency offset in [23]–[26], and it was also applied to suppress the ICI caused by time-varying channels in [27]–[32]. Recently, in [33], [34], Tchamov *et al.* directly applied the combining weights of [28] to suppress the phase noise effect.

In this paper, the CP recycling scheme is applied to suppress the ICI power incurred by phase noise. Although this idea has already been used in [33], [34], nevertheless, the heuristic combining weights adopted in [33], [34] are apparently not optimum in the sense of ICI minimization. To the best of our knowledge, the optimum combining weights have not been investigated. In this paper, we derive the optimum combining weights and provide a set of near-optimum combining weights.

Manuscript received March 13, 2013; revised July 16 and September 5, 2013. The editor coordinating the review of this paper and approving it for publication was R. Dinis.

The authors are with the Inst. of Communications Engineering, National Chiao Tung University. No. 1001 Ta Hsueh Rd., Hsinchu, Taiwan 300, R.O.C. (e-mail: ma_chun_ying.cm93@g2.nctu.edu.tw, andy1988.tw@yahoo.com.tw, huangcc@cc.nctu.edu.tw).

This work was supported by National Science Council of the Republic of China (Taiwan) under grant NSC 100-2220-E-009-025.

Digital Object Identifier 10.1109/TCOMM.2013.091513.130197

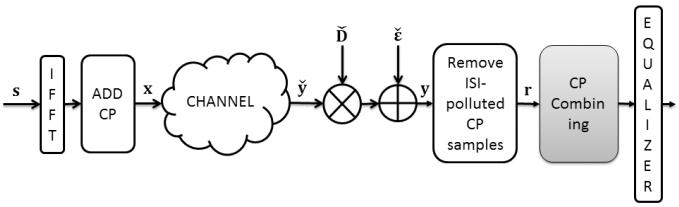


Fig. 1. Block diagram of the OFDM transceiver system model in the presence of phase noise.

Moreover, it should be noted that the proposed method can be incorporated with other phase noise mitigation methods since the output of the proposed method can be treated as a *cleaner* (or less ICI-polluted) input to the traditional phase noise mitigation methods, e.g., [8]–[14], [17]–[22].

The contributions of this paper are organized as follows: (1) we derive the optimum combining weights in the sense of ICI power minimization; (2) we propose a set of near-optimum combining weights to reduce complexity; (3) through simulations, we show that the proposed method, whose complexity is extremely low, provides about $0.5$ to $1.5$ dB gain in BER performance; (4) we systematically analyze the relationship between ICI power level and the length of CP.

Throughout this paper, we use the following notations. Boldface uppercase and lowercase letters denote matrices and vectors, respectively. The superscript $(\cdot)^T$ and $(\cdot)^H$ denote transpose and Hermitian of a matrix or vector, respectively. The superscript $(\cdot)^*$ is the conjugate of a complex variable. We use $\mathbf{x} \sim \mathcal{CN}(\boldsymbol{\mu}, \boldsymbol{\Sigma})$ to represent that $\mathbf{x}$ is a complex Gaussian distributed random vector with mean $\boldsymbol{\mu}$ and covariance matrix $\boldsymbol{\Sigma}$. $\mathbf{F}_N$ is the $N \times N$ discrete Fourier transform (DFT) matrix whose $(m,n)^{th}$ entry is given by $\frac{1}{\sqrt{N}}\exp(-\jmath\frac{2\pi mn}{N})$, with $m, n \in \{0, 1, ..., N-1\}$. We define $\text{diag}\{\mathbf{x}\}$ as a diagonal matrix with vector $\mathbf{x}$ on its diagonal. $\mathbf{1}$ is a column vector with appropriate dimension containing all ones. We use $\mathbf{O}_{M\times N}$ to represent an all-zero matrix with dimension $M \times N$. Finally, $\text{tr}(\cdot)$ denotes trace operation.

The rest of the paper is organized as follows. In Section II, the OFDM signal model and the phase noise model are presented. The proposed method is described in Section III. Subsequently, the derivations of the optimum and the near-optimum combining coefficients are presented in Section IV. Finally, simulation results and conclusion are given in Section V and VI, respectively.

## II. System Model

### A. OFDM Signal Model

The baseband system model of an OFDM system in the presence of phase noise is illustrated in Fig. 1. We use

$$\mathbf{s} = \begin{bmatrix} s(0) & s(1) & \cdots & s(N-1) \end{bmatrix}^T \tag{1}$$

to represent the transmit information symbol vector, where $N$ is the OFDM symbol length. Each entry of $\mathbf{s}$ is independently drawn from a finite alphabet $\mathcal{A}$, i.e., $s(k) \in \mathcal{A}, \quad \forall k \in [0, N-1]$. Without loss of generality, we normalize the average transmit power to unity; hence, $\mathbb{E}\left[\mathbf{s}\mathbf{s}^H\right] = \mathbf{I}_N$. To generate an ordinary OFDM symbol, the information symbol vector $\mathbf{s}$ is transformed into time domain via an $N$-point Inverse Fast Fourier Transform (IFFT) operation, and then a CP with size $N_g$ is inserted to prevent ISI. The time-domain baseband transmitter output $\mathbf{x} \triangleq \begin{bmatrix} x(-N_g) & \cdots & x(-1) & x(0) & \cdots & x(N-1) \end{bmatrix}^T$ can be mathematically described as

$$\mathbf{x} = \mathbf{T}_{\text{cp}}\mathbf{F}_N^H\mathbf{s}, \tag{2}$$

where $\mathbf{T}_{\text{cp}}$ is the CP-inserting matrix defined as

$$\mathbf{T}_{\text{cp}} = \begin{bmatrix} \mathbf{I}_{\text{cp}}^T & \mathbf{I}_N^T \end{bmatrix}^T \tag{3}$$

and $\mathbf{I}_{\text{cp}}$ is the matrix collecting the last $N_g$ rows of the identity matrix $\mathbf{I}_N$. The transmitted signal $\mathbf{x}$ is then passed through the multipath channel whose channel impulse response $\mathbf{h}$ is mathematically defined as $\begin{bmatrix} h(0) & \cdots & h(L-1) \end{bmatrix}^T$, where $L-1$ is the maximum path delay. We assume that the CP length is longer than the maximum multipath delay, that is, $N_g > L-1$. We define $\breve{\mathbf{y}} \triangleq \begin{bmatrix} \breve{y}(-N_g) & \cdots \breve{y}(N-1) \end{bmatrix}^T$ as the convolution of the transmitted signal and channel impulse response. Then, the received signal $\breve{\mathbf{y}}$ is corrupted by phase noise and Additive White Gaussian Noise (AWGN). The time-domain noise-corrupted received signal $\mathbf{y} \triangleq \begin{bmatrix} y(-N_g) & \cdots & y(N-1) \end{bmatrix}^T$ is given by

$$\mathbf{y} = \breve{\mathbf{D}}\breve{\mathbf{y}} + \breve{\boldsymbol{\varepsilon}}, \tag{4}$$

where

$$\breve{\mathbf{D}} \triangleq \text{diag}\{\begin{bmatrix} \mathrm{e}^{(\jmath\varphi(-N_g))} & \cdots & \mathrm{e}^{(\jmath\varphi(N-1))} \end{bmatrix}^T\} \tag{5}$$

is the matrix corresponding to the phase noise effect, $\varphi(n)$ is the phase noise at sample time $n$, and $\breve{\boldsymbol{\varepsilon}} \sim \mathcal{CN}(\mathbf{0}, \sigma^2\mathbf{I}_{(N+N_g)})$ is the time-domain AWGN.

At the receiver side, the first $L-1$ samples of the received signal, the so-called ISI-polluted samples, are dropped, and the remaining signal $\mathbf{r} \triangleq \begin{bmatrix} r(-N_g+L-1) & \cdots & r(N-1) \end{bmatrix}^T$, whose dimension is $(N+N_g-L+1)\times 1$, is given by

$$\mathbf{r} \triangleq \begin{bmatrix} \mathbf{O}_{(N+N_g-L+1)\times(L-1)} & \mathbf{I}_{(N+N_g-L+1)} \end{bmatrix}\mathbf{y}. \tag{6}$$

Therefore, the received signal $\mathbf{r}$ can be represented as

$$\mathbf{r} = \mathbf{D}\mathbf{H}\mathbf{x} + \boldsymbol{\varepsilon}, \tag{7}$$

where $\mathbf{D} \triangleq \text{diag}\{\begin{bmatrix} \mathrm{e}^{(\jmath\varphi(-N_g+L-1))} & \cdots & \mathrm{e}^{(\jmath\varphi(N-1))} \end{bmatrix}^T\}$,

$$\mathbf{H} = \begin{pmatrix} h(L-1) & \cdots & h(0) & 0 & \cdots & 0 \\ 0 & h(L-1) & \cdots & h(0) & \ddots & \vdots \\ \vdots & \ddots & \ddots & \ddots & \ddots & 0 \\ 0 & \cdots & 0 & h(L-1) & \cdots & h(0) \end{pmatrix}, \tag{8}$$

and $\boldsymbol{\varepsilon}$ is the vector consisting of the last $N+N_g-L+1$ elements of $\breve{\boldsymbol{\varepsilon}}$.

### B. Phase Noise Model

Phase noise is the random perturbation caused by an imperfect local oscillator. For a local oscillator with center frequency $f_c$, the oscillator output at time instant $t$ can be written as $\exp\{\jmath(2\pi f_c t + \varphi(t))\}$, where $\varphi(t)$ is the phase noise at time instant $t$. In this paper, the phase noise model recommended by IEEE 802.11ad task group [35] is used. The power spectrum

density (PSD) of the phase noise is a one-pole/one-zero model given as

$$S_\varphi(f) = K_0 \frac{1+(f/f_z)^2}{1+(f/f_p)^2}, \tag{9}$$

where $f_z$ and $f_p$ are the zero and pole frequency, respectively. In [35], the default value of each parameter is: $f_z = 100$MHz, $f_p = 1$MHz, and $K_0 = -90$dBc/Hz.

By definition, the auto-correlation function of the phase noise is the inverse Fourier transform of $S_\varphi(f)$, i.e.,

$$\rho(\tau) \triangleq \mathbb{E}[\varphi(t)\varphi(t+\tau)] = \mathcal{F}^{-1}\{S_\varphi(f)\}, \tag{10}$$

and it is derived in [21] as

$$\rho(\tau) = \frac{K_0 f_p^2}{f_z^2}\delta(\tau) + K_0 \pi f_p \left(1 - \frac{f_p^2}{f_z^2}\right) \mathrm{e}^{-2\pi f_p|\tau|}. \tag{11}$$

## III. The Proposed Method

### A. Cyclic Prefix Combining

For convenience, we define $q = N_g - L + 1$. Then, the last $q$ received samples in CP, namely $r(-q), \cdots, r(-1)$, are the so-called ISI-free samples. Since these samples are originated from the last $q$ samples of the OFDM symbol, they can be linearly combined with their corresponding OFDM samples to improve the performance. The combined signal $v_t(n)$ can be described as

$$v_t(n) = \begin{cases} r(n) & \text{, if } 0 \leqslant n \leqslant N-q-1 \\ \mu_n r(n) + \vartheta_n r(n-N) & \text{, if } N-q \leqslant n \leqslant N-1 \end{cases} \tag{12}$$

where $\{\mu_n\}_{n=N-q}^{N-1}$ and $\{\vartheta_n\}_{n=N-q}^{N-1}$ are the combining coefficients which have the following relationship

$$\mu_n = 1 - \vartheta_n, \ \forall n \in [N-q, N-1]. \tag{13}$$

The constraint (13), the so-called Nyquist constraint [24], is made to ensure the orthogonality when there is no phase noise.

After the CP combining, the combined signal $\mathbf{v}_t \triangleq [v_t(0), \cdots, v_t(N-1)]^T$ is transformed into frequency domain via an FFT operation. As a result, the frequency-domain combined signal $\mathbf{v} \triangleq [v(0), \cdots, v(N-1)]^T$ can be written as

$$\mathbf{v} = \mathbf{F}_N \mathbf{v}_t. \tag{14}$$

The CP combining operation is illustrated in Fig. 2. It should be noted that since only $q$ samples are utilized to combat phase noise, the proposed method can have a significant gain only when $q$ is a significant fraction of $N$.

### B. The Design Goal and The Solutions

The combined signal $\mathbf{v}$ can be expressed as

$$\mathbf{v} = \tilde{I}(0)\mathbf{\Lambda}\mathbf{s} + \mathbf{b} + \mathbf{z}, \tag{15}$$

where

$$\tilde{I}(0) = \frac{1}{N}\left(\sum_{m=0}^{N-q-1} \mathrm{e}^{\jmath\varphi(m)} + \sum_{n=N-q}^{N-1} (\mu_n \mathrm{e}^{\jmath\varphi(n)} + \vartheta_n \mathrm{e}^{\jmath\varphi(n-N)})\right), \tag{16}$$

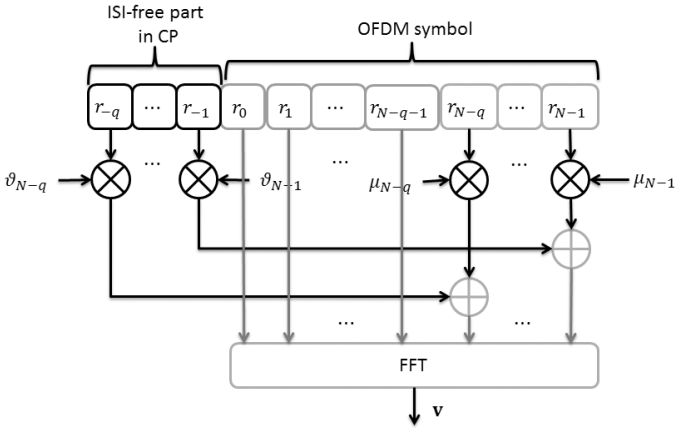


Fig. 2. Implementation of the CP combining.

is the effective common phase error (CPE) which rotates the frequency-domain received signal, $\mathbf{\Lambda} = \mathrm{diag}\{[\Lambda(0), \cdots, \Lambda(N-1)]^T\}$ represents the channel frequency response, $\mathbf{b}$ denotes the ICI term, and $\mathbf{z}$ represents the noise term. One of the major contributions of this paper is to find the optimum combining coefficients $\{\mu_n\}_{n=N-q}^{N-1}$ and $\{\vartheta_n\}_{n=N-q}^{N-1}$ that suppress the ICI power; the design goal can be mathematically described by the following optimization problem:

$$\begin{aligned} \min_{\{\mu_n\},\{\vartheta_n\}} \quad & \mathbb{E}[\mathbf{b}^H\mathbf{b}] \\ s.t. \quad & \mu_n = 1 - \vartheta_n, \ \forall n \in [N-q, N-1]. \end{aligned} \tag{17}$$

The optimum solution of (17) will be derived in Section IV. Furthermore, in order to reduce the computational complexity, a set of near-optimum combining coefficients are also derived in Section IV. The set of near-optimum combining coefficients can be explicitly written as

$$\begin{cases} \mu_n^\star = & \alpha + (N-1-n)\beta \\ \vartheta_n^\star = & 1 - \mu_n^\star \end{cases}, \ \forall n \in [N-q, N-1], \tag{18}$$

where

$$\beta = \frac{2\pi f_p T_s - 2\pi N f_p^2 T_s^2}{1 - \mathrm{e}^{-2\pi f_p N T_s} - \frac{2\pi}{3N} f_p T_s}, \tag{19}$$

$$\alpha = \frac{1}{2} - \frac{1}{2}(q-1)\beta, \tag{20}$$

and $T_s$ is the sampling period.

It is noteworthy that in (19) the calculation of $\beta$ involves only $N, T_s$ and $f_p$. In practice, the parameter $f_p$ can be obtained either by measurement or from the specifications of the VCO [11]. Since all these parameters are irrelevant to channel realizations, $\beta$ can be calculated off-line. Furthermore, the calculation of $\alpha$, $\{\mu_n\}$, and $\{\vartheta_n\}$ is extremely simple and depends only on the the size of ISI-free region $q$.

### C. Comparison with Other Windows

For convenience of comparison, we use the terminology *window* as which is used in the literature [23]–[26]. We define

$$w_n \triangleq \begin{cases} \vartheta_{N-n}, & \text{if } n \in [-q, -1] \\ 1, & \text{if } n \in [0, N-q-1] \\ \mu_n, & \text{if } n \in [N-q, N-1] \\ 0, & \text{otherwise} \end{cases} \tag{21}$$

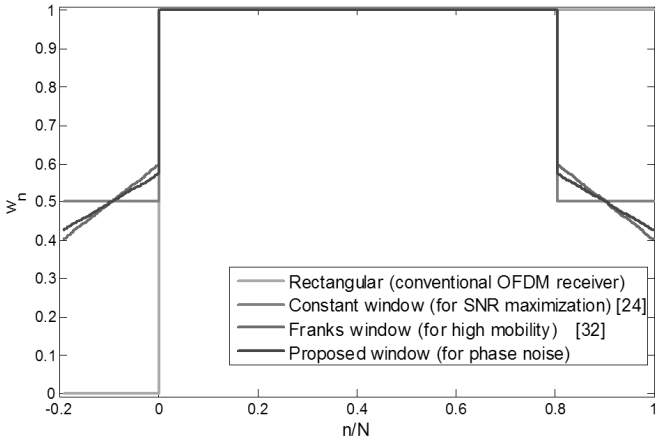


Fig. 3. Illustration of various windows with $q = 100$.

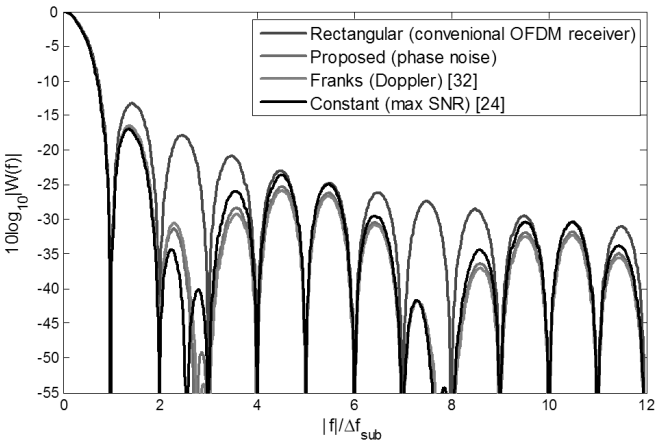


Fig. 4. Normalized frequency response of four different receiver window shapes with $q = 100$.

as the window coefficient for sample $n$. As introduced in Section I, there have been several windows, designed for different kinds of problems, in literature. Here, we briefly compare the proposed window with other windows in literature. In the following, we assume that $N = 512$ and $T_s = 37.9$ns. Fig. 3 shows each window with $q = 100$. Rectangular window represents the conventional OFDM receiver that simply removes the CP. Constant window is proven to be the maximizer of the received SNR in [24], and it was used in [28] and in [33] as a heuristic window function to mitigate Doppler-induced ICI and phase-noise-induced ICI, respectively. The Franks window, which minimizes the ICI incurred by Doppler effect, is coincidentally similar to the proposed window. In the ISI-free region, the slope of the Franks window, which minimizes the time variations of the channels, is $1/N \approx 0.002$, whereas the slope of the proposed window, which mitigates the ICI caused by the phase noise, is $\beta \approx 0.0013$.

We can also compare these windows in frequency domain. For this purpose, we introduce the normalized frequency response defined as [24]

$$W(f) = \frac{1}{N} \sum_{n=-\infty}^{\infty} w_n \mathrm{e}^{-\frac{\jmath 2\pi n(f/\Delta f_{sub})}{N}}, \tag{22}$$

where $\Delta f_{sub}$ is the subcarrier spacing. Fig. 4 shows the normalized frequency response of each window with $q = 100$. It is evident that the other three windows suppress the side lobes when compared with the rectangular window; therefore, they can be used to suppress the ICI effect. Nevertheless, they have different shapes because they are specifically designed for different kinds of ICI sources.

## IV. Derivation of the Optimum Combining Coefficients and the Near-Optimum Combining Coefficients (18)

The optimization problem (17) is difficult to solve directly; therefore, we introduce the technique originally developed for the high-mobility ICI self-cancellation technique [31] and transform the problem (17) into a tractable equivalent optimization problem.

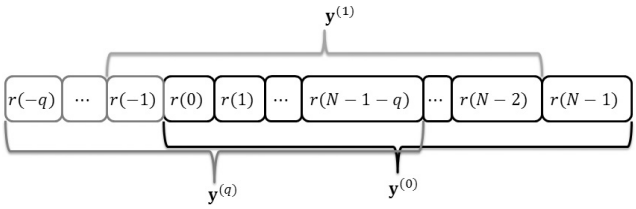


Fig. 5. Illustration of the time-domain segments.

### A. Preliminaries

For the purpose of analysis, we define received *time-domain segment* and *frequency-domain segment* as follows.

**Definition 1.** *Time-domain segment $d$, denoted as $\mathbf{y}^{(d)}$, is defined as*

$$\mathbf{y}^{(d)} = \begin{bmatrix} r(-d) & \cdots & r(N-1-d) \end{bmatrix}^T. \tag{23}$$

**Definition 2.** *Frequency-domain segment $d$, or $\mathbf{y}_F^{(d)}$, is defined as*

$$\mathbf{y}_F^{(d)} = \mathbf{F}_N \mathbf{y}^{(d)}. \tag{24}$$

Fig. 5 illustrates the relationship of each time-domain segment. Equivalently, we can rewrite (23) as

$$\mathbf{y}^{(d)} = \mathbf{R}^{(d)} \mathbf{r}, \tag{25}$$

where

$$\mathbf{R}^{(d)} = \begin{bmatrix} \mathbf{O}_{N\times(N_g-L-d)} & \mathbf{I}_N & \mathbf{O}_{N\times d} \end{bmatrix} \tag{26}$$

is the matrix that takes the desired components of $\mathbf{r}$. Moreover, from (7), we can express (25) as

$$\mathbf{y}^{(d)} = \mathbf{D}^{(d)} \mathbf{H}^{(d)} \mathbf{F}_N^H \mathbf{s} + \boldsymbol{\varepsilon}^{(d)}, \tag{27}$$

where

$$\mathbf{H}^{(d)} = \mathbf{R}^{(d)} \mathbf{H} \mathbf{T}_{\mathrm{cp}}, \tag{28a}$$

$$\boldsymbol{\varepsilon}^{(d)} = \mathbf{R}^{(d)} \boldsymbol{\varepsilon}, \tag{28b}$$

$$\mathbf{D}^{(d)} = \mathrm{diag}\{\begin{bmatrix} \mathrm{e}^{\jmath\varphi(-d)} & \cdots & \mathrm{e}^{\jmath\varphi(N-1-d)} \end{bmatrix}^T\} \tag{28c}$$

are the corresponding equivalent time-domain channel matrix, AWGN vector, and the phase noise matrix of time-domain segment $d$, respectively. Therefore, the corresponding frequency-domain segment $d$ can be written as

$$\mathbf{y}_F^{(d)} = \mathbf{F}_N \mathbf{y}^{(d)} = \mathbf{\Phi}^{(d)} \mathbf{\Lambda}^{(d)} \mathbf{s} + \mathbf{e}^{(d)}, \tag{29}$$

where

$$\mathbf{e}^{(d)} = \mathbf{F}_N \boldsymbol{\varepsilon}^{(d)}, \tag{30a}$$

$$\mathbf{\Phi}^{(d)} = \mathbf{F}_N \mathbf{D}^{(d)} \mathbf{F}_N^H, \tag{30b}$$

$$\mathbf{\Lambda}^{(d)} = \mathbf{F}_N \mathbf{H}^{(d)} \mathbf{F}_N^H \tag{30c}$$

are the frequency-domain AWGN, phase noise matrix, and channel frequency response matrix of segment $d$, respectively. To be more specific, the channel frequency response matrix is a diagonal matrix given by

$$\mathbf{\Lambda}^{(d)} = \text{diag}\{\begin{bmatrix}\Lambda^{(d)}(0) & \cdots & \Lambda^{(d)}(N-1)\end{bmatrix}^T\}, \tag{31}$$

where $\Lambda^{(d)}(k)$ is the channel frequency response on subcarrier $k$ of segment $d$, and the frequency-domain phase noise matrix $\mathbf{\Phi}^{(d)}$ is a circulant matrix which can be explicitly written as

$$\mathbf{\Phi}^{(d)} = \begin{pmatrix} I_0^{(d)} & I_1^{(d)} & \cdots & I_{N-1}^{(d)} \\ I_{N-1}^{(d)} & I_0^{(d)} & \cdots & I_{N-2}^{(d)} \\ \vdots & \ddots & \ddots & \vdots \\ I_1^{(d)} & I_2^{(d)} & \cdots & I_0^{(d)} \end{pmatrix}, \tag{32}$$

where

$$I_k^{(m)} = \frac{1}{N} \sum_{n=0}^{N-1} \exp(\jmath\varphi(n-m)) \mathrm{e}^{\frac{\jmath 2\pi nk}{N}}. \tag{33}$$

The diagonal part of $\mathbf{\Phi}^{(d)}$ will rotate the received signal constellation and cause CPE. On the other hand, the off-diagonal part of $\mathbf{\Phi}^{(d)}$ will destroy the orthogonality of OFDM and incur ICI.

### *B. Problem Reformulation, Optimum Combining Weights, and Near-Optimum Combining Weights*

In this subsection, we will reformulate the ICI minimization problem (17) as a tractable equivalent optimization problem.

The CP combining operation illustrated in Fig. 2 is equivalent to making the $q+1$ frequency-domain segments be weighted and combined. To show this equivalence, we first let $u_d$ denote the combining weight corresponding to segment $d$. Then, it can be easily verified that the weighted and combined frequency-domain signal $\mathbf{v}$ in (14) can be represented as

$$\mathbf{v} = \sum_{d=0}^{q} \mathbf{G}^{(d)} \mathbf{y}_F^{(d)} u_d \tag{34}$$

if we let

$$\mu_n = \sum_{d=0}^{N-1-n} u_d, \qquad \vartheta_n = \sum_{d=N-n}^{q} u_d, \tag{35}$$

and

$$\sum_{d=0}^{q} u_d = 1, \tag{36}$$

where

$$\mathbf{G}^{(d)} \triangleq \text{diag}\{\begin{bmatrix}\mathrm{e}^{\jmath\frac{2\pi 0d}{N}} & \mathrm{e}^{\jmath\frac{2\pi 1d}{N}} & \cdots & \mathrm{e}^{\jmath\frac{2\pi(N-1)d}{N}}\end{bmatrix}^T\} \tag{37}$$

represents the phase-shift compensation matrix that compensates the linear phase shift of each frequency-domain segment. Consequently, for the following mathematical analysis, the optimum solution is derived with respect to $\{u_d\}$ instead of $\{\mu_n\}$ and $\{\vartheta_n\}$.

We define two matrices $\mathbf{\Phi}_{\text{CPE}}^{(d)}$ and $\mathbf{\Phi}_{\text{ICI}}^{(d)}$ corresponding to the diagonal and off-diagonal parts of the matrix $\mathbf{\Phi}^{(d)}$, respectively, i.e.,

$$\mathbf{\Phi}_{\text{CPE}}^{(d)} \triangleq \text{diag}\{\begin{bmatrix}I^{(d)}(0) & \cdots & I^{(d)}(0)\end{bmatrix}^T\} = I^{(d)}(0)\mathbf{I}_N \tag{38}$$

$$\mathbf{\Phi}_{\text{ICI}}^{(d)} \triangleq \mathbf{\Phi}^{(d)} - \mathbf{\Phi}_{\text{CPE}}^{(d)}. \tag{39}$$

We also define the combining weight vector $\mathbf{u} \triangleq [u_0 \;\; u_1 \;\; \cdots \;\; u_q]^T$. Then the combined signal $\mathbf{v}$ can be expressed in a more compact form:

$$\mathbf{v} = \mathbf{m} + \mathbf{b} + \mathbf{z}, \tag{40}$$

where

$$\begin{aligned} \mathbf{m} &= \begin{bmatrix}\mathbf{G}^{(0)}\mathbf{\Phi}_{\text{CPE}}^{(0)}\mathbf{\Lambda}^{(0)}\mathbf{s} & \cdots & \mathbf{G}^{(q)}\mathbf{\Phi}_{\text{CPE}}^{(q)}\mathbf{\Lambda}^{(q)}\mathbf{s}\end{bmatrix}\mathbf{u}, \\ \mathbf{b} &= \begin{bmatrix}\mathbf{G}^{(0)}\mathbf{\Phi}_{\text{ICI}}^{(0)}\mathbf{\Lambda}^{(0)}\mathbf{s} & \cdots & \mathbf{G}^{(q)}\mathbf{\Phi}_{\text{ICI}}^{(q)}\mathbf{\Lambda}^{(q)}\mathbf{s}\end{bmatrix}\mathbf{u}, \\ \mathbf{z} &= \begin{bmatrix}\mathbf{G}^{(0)}\mathbf{e}^{(0)} & \cdots & \mathbf{G}^{(q)}\mathbf{e}^{(q)}\end{bmatrix}\mathbf{u} \end{aligned} \tag{41}$$

represent the combined signal term, ICI term, and noise term, respectively. Thus, the average ICI power is given by

$$\frac{1}{N}\mathbb{E}\left[\mathbf{b}^H\mathbf{b}\right] = \frac{1}{N}\mathbf{u}^H\mathbb{E}\left[\mathbf{C}^H\mathbf{C}\right]\mathbf{u} = \frac{1}{N}\mathbf{u}^H\mathbf{\Omega}\mathbf{u}, \tag{42}$$

where

$$\mathbf{C} \triangleq \begin{bmatrix}\mathbf{G}^{(0)}\mathbf{\Phi}_{\text{ICI}}^{(0)}\mathbf{\Lambda}^{(0)}\mathbf{s} & \cdots & \mathbf{G}^{(q)}\mathbf{\Phi}_{\text{ICI}}^{(q)}\mathbf{\Lambda}^{(q)}\mathbf{s}\end{bmatrix}, \tag{43}$$

and $\mathbf{\Omega} \triangleq \mathbb{E}[\mathbf{C}^H\mathbf{C}]$. The $(i_1, i_2)^{th}$ entry of $\mathbf{\Omega}$ can be derived as

$$\begin{aligned} &\bar{\gamma}\left[NR_\phi(0) - |i_2 - i_1|(R_\phi(0) - R_\phi(N))\right] \\ &- \bar{\gamma}\sum_{n=-N+1}^{N-1} R_\phi(n + |i_2 - i_1|)\left(1 - \frac{|n|}{N}\right), \end{aligned} \tag{44}$$

where

$$\bar{\gamma} = \frac{1}{N}\sum_{k=0}^{N-1} |\Lambda^{(0)}(k)|^2, \tag{45}$$

and $R_\phi(n)$ is the discrete-time auto-correlation function of $\exp(\jmath\varphi(n))$, which is defined as

$$R_\phi(n) \triangleq \mathbb{E}[\mathrm{e}^{\jmath\varphi(m)}(\mathrm{e}^{\jmath\varphi(m+n)})^*] = \mathbb{E}[\mathrm{e}^{\jmath(\varphi(m)-\varphi(m+n))}]. \tag{46}$$

The derivation of (44) is given in Appendix A.

Now, the ICI power minimization problem (17) can be reformulated as the following equivalent optimization problem:

$$\begin{aligned} \min_{\mathbf{u}\in\mathbb{R}^{q+1}} \quad & \mathbf{u}^T\mathbf{\Omega}\mathbf{u} \\ s.t. \quad & \mathbf{1}^T\mathbf{u} = 1. \end{aligned} \tag{47}$$

Note that $\mathbf{\Omega}$ is well-defined (each entry is given in (44)). Since (47) is a convex optimization problem, any solution that

satisfies the KKT condition is the global optimum solution [36]. The KKT condition of (47) is given as

$$\mathbf{\Omega u} = \lambda \mathbf{1}, \qquad \text{and} \qquad \mathbf{1}^T \mathbf{u} = 1, \tag{48}$$

where $\lambda$ is a Lagrange multiplier. The optimum solution $\mathbf{u}^{\Phi}$ is given by

$$\mathbf{u}^{\Phi} = \frac{\mathbf{\Omega}^{-1}\mathbf{1}}{\mathbf{1}^T\mathbf{\Omega}^{-1}\mathbf{1}} \tag{49}$$

if $\mathbf{\Omega}$ is invertible.

However, as is suggested by (49), the calculation of the optimum solution $\mathbf{u}^{\Phi}$ is quite complicated since a matrix inversion is involved. From the numerical results of (49), we approximate the optimum combining weights $\mathbf{u}^{\Phi}$ by the following explicit expression[1]

$$\mathbf{u}^{\star} = \begin{bmatrix} \alpha & \beta & \beta & \cdots & \beta & \alpha \end{bmatrix}^T, \tag{50}$$

and later we will show that

$$\alpha = \frac{1}{2} - \frac{q-1}{2}\beta \tag{51}$$

and

$$\beta = \frac{2\pi f_p T_s - 2\pi N f_p^2 T_s^2}{1 - \mathrm{e}^{-2\pi f_p N T_s} - \frac{2\pi}{3N} f_p T_s}. \tag{52}$$

It should be noted that by using the relationship (35), we can transform $\mathbf{u}^{\star}$ in (50) back to the corresponding combining coefficients $\{\mu_n^{\star}\}$ and $\{\vartheta_n^{\star}\}$ in (18). That is to say, the near-optimality of (50) infers the near-optimality of (18). In the following subsection, we will show that (50) is a near-optimum solution.

### C. Validation of the Near-Optimality of $\mathbf{u}^{\star}$ (50)

By (11) and assuming that $\varphi(n) \approx 0$, the discrete-time auto-correlation function $R_{\phi}(n)$ can be derived and approximated as

$$R_{\phi}(n) \approx 1 + \kappa_0 \mathrm{e}^{-2\pi f_p |n| T_s}, \tag{53}$$

where $\kappa_0 \triangleq K_0 \pi f_p \left(1 - f_p^2/f_z^2\right)$. By (44) and (53), the $(i_1, i_2)^{th}$ entry of $\mathbf{\Omega}$ is approximated as

$$\begin{aligned} &\bar{\gamma}\Bigg(N(1+\kappa_0) - \kappa_0 p(1 - \mathrm{e}^{-2\pi f_p N T_s}) - \\ &\sum_{n=-N+1}^{N-1} \left(1 + \kappa_0 \mathrm{e}^{-2\pi f_p |n+p| T_s}\right)\left(1 - \frac{|n|}{N}\right)\Bigg), \end{aligned} \tag{54}$$

where $p \triangleq |i_1 - i_2|$. By Taylor Series Expansion, (54) can be approximated as

$$\begin{aligned} &\bar{\gamma}N(1+\kappa_0) - \bar{\gamma}\kappa_0 p(1 - \mathrm{e}^{-2\pi f_p N T_s}) - \sum_{n=-N+1}^{N-1} \bar{\gamma}\Bigg(1 + \kappa_0 \\ &- 2\kappa_0 \pi f_p T_s |n+p| + 2\kappa_0 \pi^2 f_p^2 T_s^2 (n+p)^2\Bigg)\left(1 - \frac{|n|}{N}\right). \end{aligned} \tag{55}$$

[1]This approximation is only valid for the IEEE 802.11ad phase noise model [35] and Wiener phase noise model, whereas the optimum solution $\mathbf{u}^{\Phi}$ given by (49) is valid for all kinds of phase noise sources. Therefore, for a general phase noise process, the optimum combining weights can be calculated via (49) and (44).

For brevity, (55) can be expressed as

$$\begin{aligned} &C_1 - \kappa_1 p + \kappa_2 \underbrace{\sum_{n=-N+1}^{N-1} |n+p| \left(1 - \frac{|n|}{N}\right)}_{(a)} \\ &- \kappa_3 \underbrace{\sum_{n=-N+1}^{N-1} (n+p)^2 \left(1 - \frac{|n|}{N}\right)}_{(b)}, \end{aligned} \tag{56}$$

where

$$C_1 = \bar{\gamma}(1+\kappa_0)\left(N - \sum_{n=-N+1}^{N-1}\left(1 - \frac{|n|}{N}\right)\right), \tag{57}$$

$$\kappa_1 = (1 - \mathrm{e}^{-2\pi f_p N T_s})\bar{\gamma}\kappa_0, \tag{58}$$

$$\kappa_2 = 2\pi f_p T_s \bar{\gamma}\kappa_0, \tag{59}$$

and

$$\kappa_3 = 2\pi^2 f_p^2 T_s^2 \bar{\gamma}\kappa_0. \tag{60}$$

We remove the absolute value operations of $(a)$ in (56), and then $(a)$ can be derived as

$$\begin{aligned} (a) &= \sum_{n=-N+1}^{-p} |n+p| \left(1 - \frac{|n|}{N}\right) + \sum_{-p+1 \leqslant n \leqslant 0} |n+p| \left(1 - \frac{|n|}{N}\right) \\ &\quad + \sum_{n=1}^{N-1} |n+p| \left(1 - \frac{|n|}{N}\right) \\ &= \sum_{n=p}^{N-1} (n-p)\left(1 - \frac{n}{N}\right) - \sum_{0 \leqslant n \leqslant p-1} (n-p)\left(1 - \frac{n}{N}\right) \\ &\quad + \sum_{n=1}^{N-1} (n+p)\left(1 - \frac{n}{N}\right). \end{aligned} \tag{61}$$

Furthermore, $(a)$ in (56) can be rearranged as a polynomial function of $p$, given as

$$\begin{aligned} (a) &= 2\sum_{n=1}^{N-1} n\left(1 - \frac{n}{N}\right) - 2\sum_{1 \leqslant n \leqslant p-1} (n-p)\left(1 - \frac{n}{N}\right) + p \\ &= C_2 - \frac{1}{3N}p^3 + p^2 + \frac{1}{3N}p, \end{aligned} \tag{62}$$

where $C_2$ is a constant. Similarly, we remove the absolute value operations of $(b)$ in (56) and derive $(b)$ as

$$\begin{aligned} (b) &= \sum_{n=-N+1}^{N-1} (n+p)^2 \left(1 - \frac{|n|}{N}\right) \\ &= \sum_{n=-N+1}^{-1} (n+p)^2 \left(1 + \frac{n}{N}\right) + p^2 + \sum_{n=1}^{N-1} (n+p)^2 \left(1 - \frac{n}{N}\right) \\ &= C_3 + Np^2, \end{aligned} \tag{63}$$

where $C_3$ is a constant. By (62) and (63), we can rewrite (56) as a polynomial function of $p$ as

$$C_4 + bp + cp^2 - \frac{\kappa_2}{3N}p^3, \tag{64}$$

where

$$b = \frac{1}{3N}\kappa_2 - \kappa_1, \tag{65}$$

$$c = \kappa_2 - N\kappa_3, \tag{66}$$

and $C_4$ is a constant. In practice, the third-order term of (64), namely, $\kappa_2/(3N)p^3$, can be neglected due to the following two reasons: (1) For most practical wireless communication systems, $\kappa_2/(3N) \ll c$, e.g., for IEEE 802.11ad specification $\kappa_2/(3N) \approx 1.5 \times 10^{-6}$ and $c \approx 9.3 \times 10^{-4}$. (2) In practice, the ISI-free region $q$ is quite small such that the gap between $p^3$ and $p^2$ is not large enough to compensate for the difference produced by their corresponding coefficients. Hence, (64) can be approximated as

$$C_4 + bp + cp^2. \tag{67}$$

In summary, we have shown that $\mathbf{\Omega}$ can be approximated by

$$\mathbf{\Omega} \approx \begin{bmatrix} f(0) & f(1) & \cdots & f(q) \\ f(1) & f(0) & \ddots & f(q-1) \\ \vdots & \ddots & \ddots & \vdots \\ f(q) & f(q-1) & \cdots & f(0) \end{bmatrix}, \tag{68}$$

where

$$f(p) = C_4 + bp + cp^2, \ \forall p \in [0, q]. \tag{69}$$

By (68) and (50), the $i^{th}$ element of $\mathbf{\Omega u}^\star$ equals to

$$\alpha\big(f(i) + f(q-i)\big) + \beta\left(\sum_{m=1-i}^{q-i-1} f(|m|)\right). \tag{70}$$

Eq. (70) can be further derived as

$$\begin{aligned} &\alpha\big[bi + ci^2 + b(q-i) + c(q-i)^2\big] \\ &+ \beta\sum_{m=1-i}^{q-i-1}\big(b|m| + cm^2\big) + C_5 \\ =&\alpha c(2i^2 - 2qi) + \beta b\sum_{m=1-i}^{q-i-1}|m| + \beta c\sum_{m=1-i}^{q-i-1} m^2 + C_6 \\ =&i(i-q)\left[2\alpha c + \beta b - \beta c + \beta cq\right] + C_7, \end{aligned} \tag{71}$$

where $C_5, C_6$, and $C_7$ are all constants. It is implied by the condition $\mathbf{\Omega u}^\star = \lambda\mathbf{1}$ that

$$2\alpha c + \beta b - \beta c + \beta cq = 0. \tag{72}$$

Similarly, from the other condition $\mathbf{1}^T\mathbf{u}^\star = 1$, we can conclude that

$$2\alpha + (q-1)\beta = 1. \tag{73}$$

From (72) and (73), we can derive that

$$\begin{aligned} \alpha =& \frac{1}{2} + \frac{c}{2b}(q-1) = \frac{1}{2} - \frac{q-1}{2}\beta \\ \beta =& -\frac{c}{b} = \frac{2\pi f_p T_s - 2\pi N f_p^2 T_s^2}{1 - \mathrm{e}^{-2\pi f_p N T_s} - \frac{2\pi}{3N} f_p T_s}. \end{aligned} \tag{74}$$

As a result, we have shown that (50) is approximately the optimum solution since the KKT condition (48) approximately holds. Equivalently, the near-optimality of (18) is validated as well.

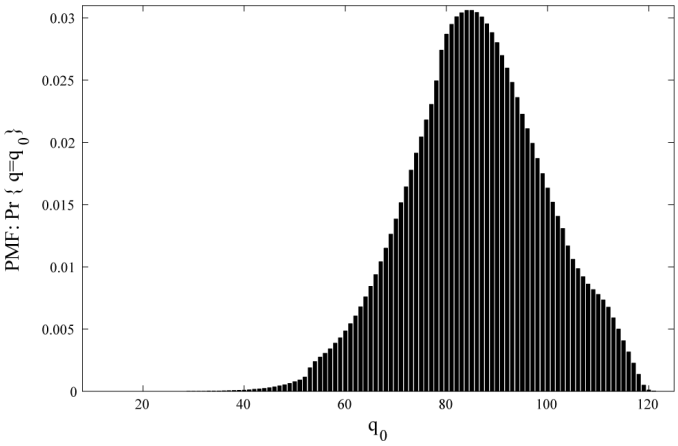


Fig. 6. The PMF of $q$.

TABLE I
SIMULATION PARAMETERS.

| | | | |
|---|---|---|---|
| Sample Rate | 2.64GHz | CP Length | 128 |
| Carrier Frequency | 60 GHz | # of Data Subcarriers | 336 |
| Subcarrier Spacing | 5.15625MHz | # of Pilot Subcarriers | 16 |
| FFT Length | 512 samples | # of DC Subcarriers | 3 |

## V. Simulation Results

### A. Simulation Parameters

Our simulation parameters are mainly based on the specification proposed by IEEE 802.11ad task group [37]. The simulation parameters are listed in Table I. We define $\mathcal{P}$ as the pilot index set, and the details of $\mathcal{P}$ are defined in [37].

The channel is simulated according to the IEEE 802.11ad 60GHz channel model [38]; specifically, conference room STA-STA sub-scenario is applied, and we use the default setting of [38] throughout our simulations. In this channel model [38], the channel realizations are generated based on a ray-tracing algorithm which takes the 60GHz electromagnetic waves propagation properties into account. In the conference room STA-STA sub-scenario, a $4.5\text{m}\times$ $3\text{m}\times$ $3\text{m}$ conference room is considered, and both the transmitter and the receiver are located on a table in the center of the room. For each channel realization, the positions of the transmitter and the receiver are both uniformly distributed on the top of the table. Additionally, each transceiver equips a steerable directional antenna, whose half-power antenna beamwidth is $30^\circ$. For more details, please refer to [38]. We execute a Monte Carlo experiment to get the probability mass function (PMF) of the number of ISI-free samples, namely $q$, for this channel. The PMF of $q$ is shown in Fig. 6. The expected value of $q$ is 84.9, and the standard deviation of $q$ is $13.44$.

The phase noise model used is based on [35], as described in section II, and each parameter is set to its default value in [35].

### B. Assumptions in Simulations

We assume that channel is static within a period containing $40$ OFDM symbols. Each simulation result is averaged over $5000$ independent channel realizations. We assume that there

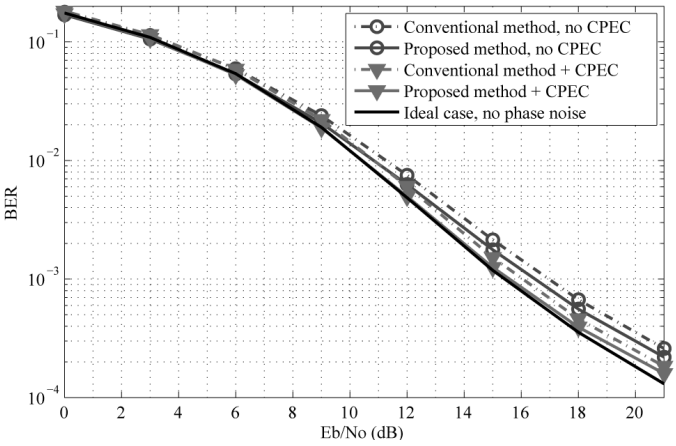


Fig. 7. BER performance of 16QAM OFDM in the presence of phase noise.

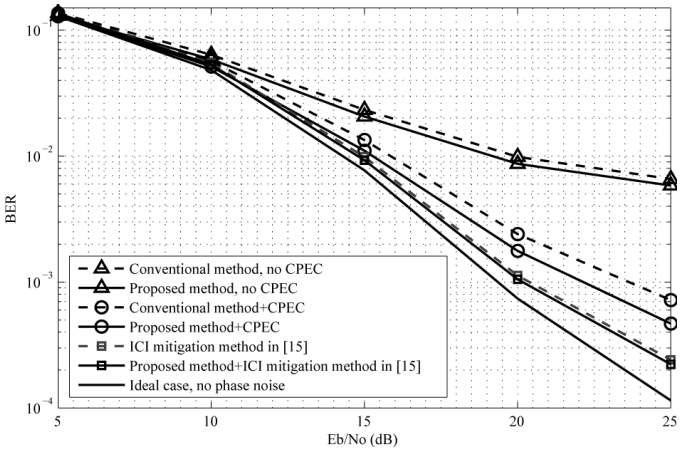


Fig. 8. BER performance of 64QAM OFDM in the presence of phase noise.

is a preamble in each OFDM data frame, and by utilizing the preamble, the channel frequency response $\mathbf{\Lambda}$ can be accurately estimated via a channel estimation method robust against phase noise effect, e.g., [11]–[14], [17], [18]. For simplicity, we assume that the channel frequency response is *perfectly estimated*.

We apply the method proposed in [8] to estimate the CPE. According to [8], the CPE is estimated as

$$\hat{I}(0) = \frac{\sum\limits_{k\in\mathcal{P}} v(k)s^*(k)\tilde{\Lambda}^*(k)}{\sum\limits_{k\in\mathcal{P}} |s(k)\tilde{\Lambda}(k)|^2}. \tag{75}$$

Note that in [8] the CPE can be iteratively updated via the help of the detected data. For simplicity, we do not use the iterative estimator in this paper. After CPE estimation, the combined signal $\mathbf{v}$ is fed into a CPE compensator (CPEC), a one-tap equalizer, and a data detector; the aforementioned process can be mathematically described as

$$\hat{\mathbf{s}} = \Pi\left(\frac{\tilde{\mathbf{\Lambda}}^{-1}\mathbf{v}}{\hat{I}(0)}\right), \tag{76}$$

where $\Pi(\cdot)$ is an entry-wise quantization function which quantizes each entry to its nearest constellation point, and $\hat{\mathbf{s}}$ is the detected data. It is worth mentioning that almost all ICI cancellation methods (e.g., [8]–[22], [33], [34]) can be applied to further mitigate the residual ICI.

### C. Simulation Results

The BER performance for OFDM transmissions employing 16QAM modulation in the presence of phase noise is plotted in Fig. 7. For brevity, the method without CP combining is called "*conventional method*" in the following. We compare the BER performance of the conventional method and the proposed method with and without CPEC in this figure. The bottom curve is the phase-noise-free case, which serves as the ideal case. As shown from the figure, we observe that the performance of the proposed method is indistinguishable from the ideal case for $E_b/N_0$ less than 17dB. And the performance of the proposed method is about 0.5dB better than the conventional method at the BER levels being equal to $10^{-2}$ and $10^{-3}$.

Similarly, Fig. 8 shows the BER performance of 64QAM OFDM transmissions in the presence of phase noise. Without CPEC, both the proposed method and the conventional method exhibit an error floor. Nevertheless, the proposed method outperforms the conventional method and has about 1dB gain at the BER level $10^{-2}$. When CPEC is included, the error floor effect is extensively improved. In this situation, it is observed that the proposed method still outperforms the conventional method. For example, with BER being equal to $10^{-3}$, the proposed method is about 1.5dB better than the conventional method. However, in this case, the performance gap between the ideal case and the proposed method is evident because the ICI effect is more severe for 64QAM. As mentioned earlier, the proposed method can be in conjunction with other ICI mitigation methods to further improve BER performance. Here we use the ICI mitigation method described in [15] as an example. As shown in Fig. 8, the performance is greatly improved via using the method proposed in [15]. In this case, the proposed method still provides an observable performance improvement, e.g., it has a 0.3dB gain at the BER level $10^{-3}$. It is worth mentioning that the aforementioned performance improvements resulted from the proposed method, although not large, is remarkable because the proposed method is extremely simple.

The coded BER performance of 16QAM and 64QAM are shown in Fig. 9(a) and Fig. 9(b), respectively. The LDPC code with code rate $1/2$ defined by IEEE 802.11ad specification [37] is used in simulations. For simplicity, the traditional Bit Flipping (BF) algorithm is used to decode the LDPC code. In Fig. 9(a) and Fig. 9(b), a specific channel realization, which is a typical channel realization drawn from the random channel generator [38]. The considered specific channel realization is given as $[-0.02527 - \jmath 0.12424, -0.00878 + \jmath 0.04851, 0.246 + \jmath 0.08669, -0.87908 - \jmath 0.3457, 0.00258 - \jmath 0.00365, -0.01489 - \jmath 0.0798, -0.05142 + \jmath 0.0956]$, and the corresponding lags are $[0, 2, 9, 20, 22, 37, 39]$ samples, respectively. From Fig. 9(a) and Fig. 9(b), it is observed that the proposed method clearly outperforms the conventional method when error control coding is included.

Fig. 10 shows the BER performance as a function of phase noise severity, and here we apply the Wiener phase noise

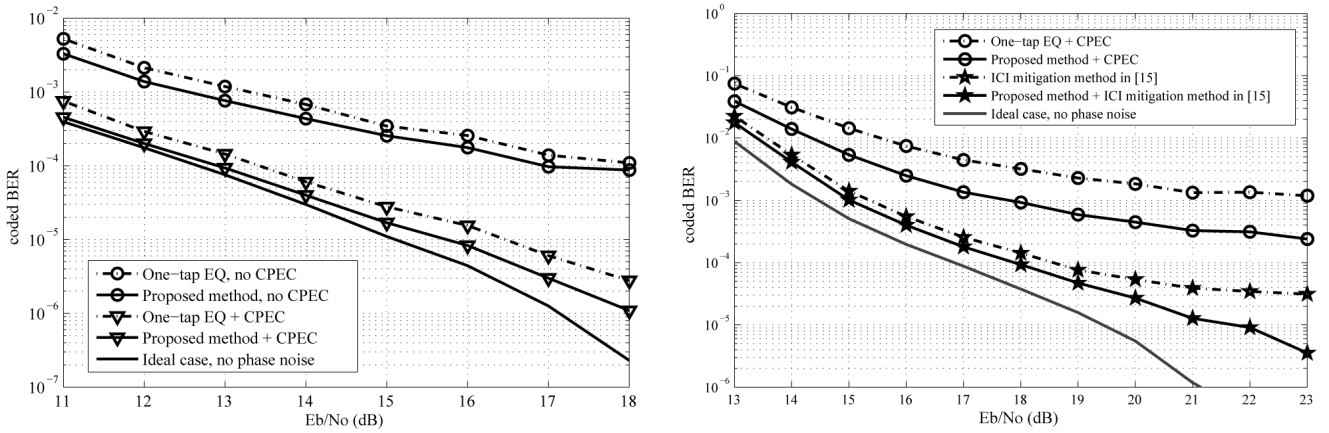


(a) Coded BER performance of 16QAM

(b) Coded BER performance of 64QAM

Fig. 9. The coded-BER performance in the presence of phase noise.

model instead of the phase noise model described in Section II. Besides the phase noise model used in this paper, Wiener phase noise is another commonly used model for a free-running oscillator [1]–[5], [7]–[10], [14]–[20]. In general, the Wiener phase noise process $\varphi(n)$ can be described as

$$\varphi(n) = \varphi(n-1) + \xi(n), \tag{77}$$

where $\xi(n) \sim \mathcal{N}(4\pi\Delta f_{3dB}T_s)$ and $\Delta f_{3dB}$ is the one-sided 3dB linewidth of the Wiener process [1]. It can be easily proven that the proposed method can be directly applied to the Wiener phase noise except that the pole frequency $f_p$ should be substituted by $\Delta f_{3dB}$. In Fig. 10, the relative phase noise linewidth $\delta_{PN}$ is defined as $\Delta f_{3dB}/\Delta f_{sub}$ [19]. It is evident that the BER of the proposed method is always lower than or indistinguishable from the conventional method. For $\delta_{PN}$ being small enough, $10^{-6}$ for example, the BER of the conventional method almost merges with the ideal case. Surprisingly, the BER of the proposed method is lower than the phase-noise-free case when $\delta_{PN} < 3 \times 10^{-5}$. This is because the proposed method utilizes the CP information, which is simply discarded in the phase-noise-free case. The CP compensation method suppresses not only the ICI power caused by phase noise but also the thermal noise power. That is to say,

$$\mathbb{E}[\|\mathbf{z}\|^2] < \sigma^2. \tag{78}$$

The proof of (78) is given in Appendix B.

Fig. 11 shows the percentage of the reduction in ICI power, which serves as a metric to evaluate the ICI suppression capability, as a function of $q$. The formal definition of the percentage of the reduction in ICI power is

$$\left[1 - \frac{\mathbf{u}^T\mathbf{\Omega}\mathbf{u}}{\mathbf{i}^T\mathbf{\Omega}\mathbf{i}}\right] \ (\%), \tag{79}$$

where $\mathbf{i} \triangleq \begin{bmatrix}1 & 0 & \cdots & 0\end{bmatrix}^T$. In [33], [34], the combining weights of [28] were applied to suppress the ICI caused by phase noise. The ICI suppression capability of the combining weights [28], denoted as *Svensson's weights*, is compared with that of the proposed optimum and near-optimum weights in Fig. 11. The phase noise model introduced in Section II is used here. Since this metric is not dependent on channel

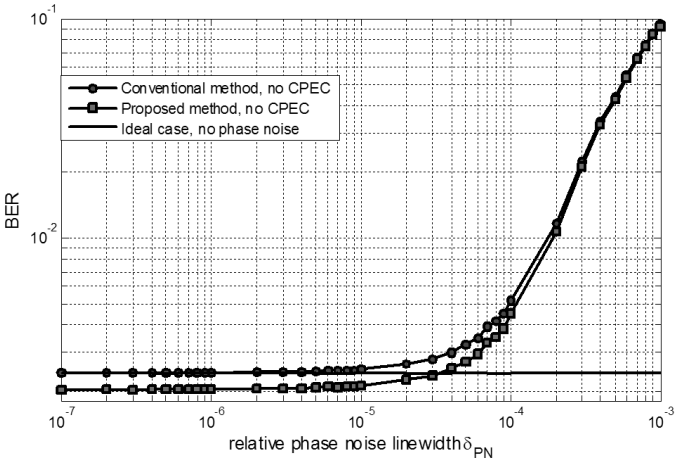


Fig. 10. OFDM BER performance for a free-running oscillator as a function of relative phase noise linewidth $\delta_{PN}$ (QPSK, $E_b/N_0 = 10$dB).

realizations for a fixed $q$ value, we do not assume any specific channel model. From Fig. 11, we observe the following facts. First, it is obvious that we can reduce the ICI power to an acceptable level by extending the length of CP. In other words, we can make a trade-off between spectral efficiency and the ICI power induced by phase noise. As shown in Fig. 11(a), the ICI power can be effectively suppressed at the expense of the loss in spectral efficiency, e.g., for $q = N/4$ the reduction in ICI power is about $20\%$. Taking $q = N$ for another example, the ICI power is reduced more than half in this situation, which means that a *repetition-code-like* transmission scheme[2] can effectively reduce the ICI power incurred by phase noise. Second, from Fig. 11(a), we can observe that the proposed optimum and near-optimum combining weights clearly outperform Svensson's weights, especially for $q \geqslant 200$. Third, the proposed near-optimum weights have a evident performance gap while $q$ approaches $N$. The reason is that we have made an approximation in (64) that the third order term is negligibly small, which is only valid when $q$ is much

[2]Traditional transmission schemes such as OFDM [27], single carrier block transmission (SCBT), and code-division multiple access (CDMA) can be transmitted in such a manner.

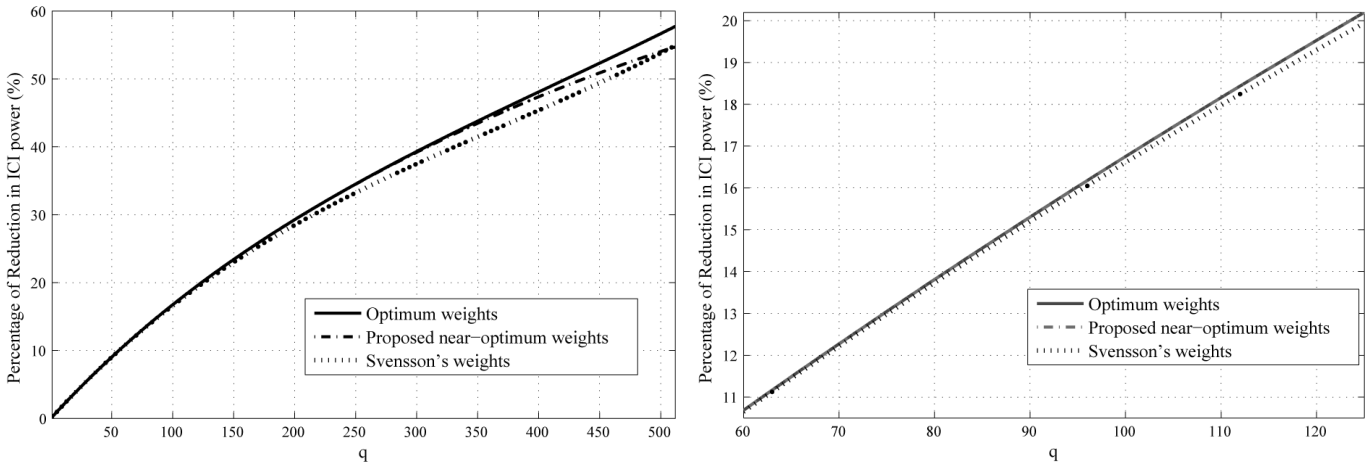


(a) $q = 1, \cdots, 512$ (b) A zoom-in section

Fig. 11. The percentage of the reduction in ICI power as a function of $q$.

smaller than $N$. However, for a reasonable value of $q$, the performance of the proposed near-optimum weights is almost identical to that of the optimum weights. Last, as shown in Fig. 6, for the simulation channels used in this paper, $q$ usually ranges from $40$ to $60$. Hence, we provide a zoom-in section in Fig. 11(b) so that we can focus on the ICI suppression capability of each method for the range of $q$ in which we are interested. As shown in Fig. 11(b), the performance of the proposed near-optimum weights is indistinguishable from that of the optimum weights, and the proposed weights clearly outperform Svensson's weights. Even though the performance improvement is not tremendous, we still recommend to use the proposed near-optimum weights rather than Svensson's weights, for they have essentially the same complexity.

## VI. Conclusion

In this paper, a simple and effective ICI suppression method in the presence of phase noise for OFDM transmission is proposed. The method is based on the utilization of the ISI-free samples in CP, which are traditionally abandoned. We derive the optimum combining coefficients for ICI power minimization and propose a set of near-optimum combining coefficients for complexity reduction. Simulation results show that the proposed method is about $0.5$ to $1.5$dB better than the conventional method with negligible amount of additional computation complexity. This paper validates the fact that an additional performance gain can be achieved by properly exploiting the unused resources in CP.

## Appendix A
## The Derivations of (44)

Through (42) and (43), we can rewrite the $(i_1, i_2)^{th}$ entry of $\mathbf{\Omega}$ as

$$\mathbb{E}\left[\mathbf{s}^H \mathbf{\Lambda}^{(i_1)H} \mathbf{\Phi}_{\text{ICI}}^{(i_1)H} \mathbf{G}^{(i_1)H} \mathbf{G}^{(i_2)} \mathbf{\Phi}_{\text{ICI}}^{(i_2)} \mathbf{\Lambda}^{(i_2)} \mathbf{s}\right] \tag{80a}$$

$$= \text{tr}\left(\mathbb{E}\left[\mathbf{s}^H \mathbf{\Lambda}^{(i_1)H} \mathbf{\Phi}_{\text{ICI}}^{(i_1)H} \mathbf{G}^{(i_1)H} \mathbf{G}^{(i_2)} \mathbf{\Phi}_{\text{ICI}}^{(i_2)} \mathbf{\Lambda}^{(i_2)} \mathbf{s}\right]\right) \tag{80b}$$

$$= \text{tr}\left(\mathbb{E}\left[\mathbf{\Lambda}^{(i_1)H} \mathbf{\Phi}_{\text{ICI}}^{(i_1)H} \mathbf{G}^{(i_1)H} \mathbf{G}^{(i_2)} \mathbf{\Phi}_{\text{ICI}}^{(i_2)} \mathbf{\Lambda}^{(i_2)} \mathbf{s}\mathbf{s}^H\right]\right) \tag{80c}$$

$$= \text{tr}\left(\mathbb{E}\left[\mathbf{\Phi}_{\text{ICI}}^{(i_1)H} \mathbf{G}^{(i_1)H} \mathbf{G}^{(i_2)} \mathbf{\Phi}_{\text{ICI}}^{(i_2)}\right] \mathbf{\Lambda}^{(i_2)} \mathbf{\Lambda}^{(i_1)H}\right). \tag{80d}$$

From (80a) to (80b), we use the fact that (80a) is a scalar, hence it is equal to its trace. To derive (80c) from (80b), we use the equality $\text{tr}(\mathbf{AB}) = \text{tr}(\mathbf{BA})$. Since we assume $\mathbb{E}[\mathbf{s}\mathbf{s}^H] = \mathbf{I}_N$, together with the equality $\text{tr}(\mathbf{AB}) = \text{tr}(\mathbf{BA})$, we get (80d). For convenience, we define

$$\mathbf{K} \triangleq \mathbf{\Lambda}^{(0)} \mathbf{\Lambda}^{(0)H}. \tag{81}$$

Hence, $\mathbf{\Lambda}^{(v)} \mathbf{\Lambda}^{(r)H} = \mathbf{K}\mathbf{G}^{(r-v)}$. So, (80d) becomes

$$\text{tr}\left(\mathbb{E}[\mathbf{\Phi}_{\text{ICI}}^{(i_1)H} \mathbf{G}^{(i_2-i_1)} \mathbf{\Phi}_{\text{ICI}}^{(i_2)}] \mathbf{K}\mathbf{G}^{(i_1-i_2)}\right). \tag{82}$$

Since $\mathbf{\Phi}_{\text{ICI}}^{(i_1)} = \mathbf{\Phi}^{(i_1)} - \mathbf{\Phi}_{\text{CPE}}^{(i_1)}$, (82) can be divided into the following four terms

$$\text{tr}\left(\mathbb{E}\left[\mathbf{\Phi}^{(i_1)H} \mathbf{G}^{(i_2-i_1)} \mathbf{\Phi}^{(i_2)} \mathbf{K}\mathbf{G}^{(i_1-i_2)}\right]\right) \tag{83a}$$

$$-\text{tr}\left(\mathbb{E}\left[\mathbf{\Phi}_{\text{CPE}}^{(i_1)H} \mathbf{G}^{(i_2-i_1)} \mathbf{\Phi}^{(i_2)} \mathbf{K}\mathbf{G}^{(i_1-i_2)}\right]\right) \tag{83b}$$

$$-\text{tr}\left(\mathbb{E}\left[\mathbf{\Phi}^{(i_1)H} \mathbf{G}^{(i_2-i_1)} \mathbf{\Phi}_{\text{CPE}}^{(i_2)} \mathbf{K}\mathbf{G}^{(i_1-i_2)}\right]\right) \tag{83c}$$

$$+\text{tr}\left(\mathbb{E}\left[\mathbf{\Phi}_{\text{CPE}}^{(i_1)H} \mathbf{G}^{(i_2-i_1)} \mathbf{\Phi}_{\text{CPE}}^{(i_2)} \mathbf{K}\mathbf{G}^{(i_1-i_2)}\right]\right). \tag{83d}$$

By (30b), the first term (83a) can be expressed as

$$\begin{aligned}&(83a)\\ &= \text{tr}\left(\mathbf{G}^{(i_1-i_2)} \mathbf{F}\mathbb{E}[\mathbf{D}^{(i_1)H} \mathbf{F}^H \mathbf{G}^{(i_2-i_1)} \mathbf{F}\mathbf{D}^{(i_2)}] \mathbf{F}^H \mathbf{K}\right)\\ &= \frac{1}{N} \sum_{k=0}^{N-1} |\Lambda^{(0)}(k)|^2 \left[(N - |i_1 - i_2|) R_\phi(0) + |i_1 - i_2| R_\phi(N)\right].\end{aligned} \tag{84}$$

The second term (83b) equals to

$$\begin{aligned}
&\mathrm{tr}\left(\mathbb{E}[\mathbf{G}^{(i_1-i_2)}\mathbf{\Phi}_{\mathrm{CPE}}^{(i_1)H}\mathbf{G}^{(i_2-i_1)}\mathbf{\Phi}^{(i_2)}]\mathbf{K}\right)\\
&=\mathrm{tr}\left(\mathbb{E}[\mathbf{\Phi}_{\mathrm{CPE}}^{(i_1)H}\mathbf{\Phi}^{(i_2)}]\mathbf{K}\right)\\
&=\mathrm{tr}\left(\mathbb{E}\left[\begin{pmatrix} I_0^{(i_1)} & & \mathbf{O}\\ & \ddots & \\ \mathbf{O} & & I_0^{(i_1)}\end{pmatrix}^H\begin{pmatrix} I_0^{(i_2)} & \times & \times\\ \times & \ddots & \times\\ \times & \times & I_0^{(i_2)}\end{pmatrix}\right]\mathbf{K}\right)\\
&=\frac{1}{N^2}\sum_{m=0}^{N-1}\sum_{n=0}^{N-1}R_\phi(m-n+|i_2-i_1|)\mathrm{tr}(\mathbf{K})\\
&=\frac{\bar\gamma}{N}\cdot\Big[\sum_{n=1}^{N-1}\Big(R_\phi(n+|i_2-i_1|)\\
&+R_\phi(-n+|i_2-i_1|)\Big)(N-n)+NR_\phi(|i_2-i_1|)\Big],
\end{aligned}\tag{85}$$

where '$\times$' stands for '*don't care*'. The first equality holds because $\mathbf{\Phi}_{\mathrm{CPE}}^{(i_2)}$, $\mathbf{G}^{(i_2-i_1)}$, and $\mathbf{G}^{(i_1-i_2)}$ are all diagonal matrix so that they are interchangeable in matrix multiplications. Hence $\mathbf{G}^{(i_2-i_1)}$ and $\mathbf{G}^{(i_1-i_2)}$ cancels with each other.

The third term (83c) equals to

$$\begin{aligned}
&\mathrm{tr}\left(\mathbb{E}[\mathbf{\Phi}^{(i_1)H}\mathbf{\Phi}_{\mathrm{CPE}}^{(i_2)}]\mathbf{K}\right)\\
=&\mathrm{tr}\left(\mathbb{E}\left[\begin{pmatrix} I_0^{(i_1)} & \times & \times\\ \times & \ddots & \times\\ \times & \times & I_0^{(i_1)}\end{pmatrix}^H\begin{pmatrix} I_0^{(i_2)} & & \mathbf{O}\\ & \ddots & \\ \mathbf{O} & & I_0^{(i_2)}\end{pmatrix}\mathbf{K}\right]\right).
\end{aligned}\tag{86}$$

The last term (83d) equals to

$$\begin{aligned}
&\mathrm{tr}\left(\mathbb{E}[\mathbf{\Phi}_{\mathrm{CPE}}^{(i_1)H}\mathbf{\Phi}_{\mathrm{CPE}}^{(i_2)}]\mathbf{K}\right)\\
=&\mathrm{tr}\left(\mathbb{E}\left[\begin{pmatrix} I_0^{(i_1)} & & \mathbf{O}\\ & \ddots & \\ \mathbf{O} & & I_0^{(i_1)}\end{pmatrix}^H\begin{pmatrix} I_0^{(i_2)} & & \mathbf{O}\\ & \ddots & \\ \mathbf{O} & & I_0^{(i_2)}\end{pmatrix}\mathbf{K}\right]\right).
\end{aligned}\tag{87}$$

Apparently, both (86) and (87) are identical to (85). Hence, the $(i_1,i_2)^{th}$ entry of $\mathbf{\Omega}$ equals to

$$\begin{aligned}
&\bar\gamma\Big[(N-|i_2-i_1|)\cdot R_\phi(0)+|i_2-i_1|\cdot R_\phi(N)-R_\phi(|i_2-i_1|)\Big]\\
&-\frac{\bar\gamma}{N}\sum_{n=1}^{N-1}\Big[R_\phi(n+|i_2-i_1|)+R_\phi(-n+|i_2-i_1|)\Big]\cdot(N-n).
\end{aligned}\tag{88}$$

By simple mathematics, (88) can be rewritten as

$$\begin{aligned}
&\bar\gamma\big[NR_\phi(0)-|i_2-i_1|(R_\phi(0)-R_\phi(N))\big]\\
&-\bar\gamma\sum_{n=-N+1}^{N-1}R_\phi(n+|i_2-i_1|)\left(1-\frac{|n|}{N}\right).
\end{aligned}\tag{89}$$

## APPENDIX B
## PROOF OF $\mathbb{E}[\|\mathbf{z}\|^2]<\sigma^2$

By [31], for a given combining weight vector $\mathbf{u}$, the combined noise power is given as

$$\mathbb{E}[\|\mathbf{z}\|^2]=\mathbf{u}^T\mathbf{\Psi}\mathbf{u},\tag{90}$$

where

$$\mathbf{\Psi}=\frac{\sigma^2}{N}\begin{pmatrix} N & N-1 & \dots & N-q\\ N-1 & N & \dots & N-q+1\\ \vdots & \vdots & \ddots & \vdots\\ N-q & N-q+1 & \dots & N\end{pmatrix}.\tag{91}$$

By applying (50) into (91), we have

$$\begin{aligned}
&\frac{N}{\sigma^2}\mathbb{E}[\mathbf{u}^{\star T}\mathbf{\Psi}\mathbf{u}^\star]\\
=&2\alpha^2+2\alpha\beta N(q-1)+\alpha\beta(2N-q)(q-1)+\beta^2N(q-1)^2\\
&-\beta^2\left(qN+2\sum_{i=1}^{q}(q-i)(N-i)\right)-\alpha\beta q(q-1)\\
<&2\alpha^2+2\alpha\beta N(q-1)+\alpha\beta(2N-q)(q-1)+\beta^2N(q-1)^2\\
=&N-\frac{1}{2}q\left[1-(q-1)\beta\right]
\end{aligned}\tag{92}$$

In practice, $1-(q-1)\beta>0$; therefore, we can conclude that $\mathbf{u}^{\star T}\mathbf{\Psi}\mathbf{u}^\star<\sigma^2$. ■

## ACKNOWLEDGMENT

The authors would like to thank anonymous reviewers and the Editor for their constructive advices and comments that help improve this paper.

## REFERENCES

[1] T. Pollet, M. Van Bladel, and M. Moeneclaey, "BER sensitivity of OFDM systems to carrier frequecy offset and Wiener phase noise," *IEEE Trans. Commun.*, vol. 43, no. 2/3/4, pp. 191–193, Feb. 1995.

[2] P. Robertson and S. Kaiser, "Analysis of the effects of phase-noise in orthogonal frequency division multiplex (OFDM) systems," in *Proc. 1995 IEEE International Conf. Commun.*, vol. 3, pp. 1652–1657.

[3] L. Tomba, "On the effect of Wiener phase noise in OFDM systems," *IEEE Trans. Commun.*, vol. 46, no. 5, pp. 580–583, May 1998.

[4] A. G. Armada, " Understanding the effects of phase noise in orthogonal frequency division multiplexing (OFDM)," *IEEE Trans. Broadcast.*, vol. 47, no. 2, pp. 153–159, Jun. 2001.

[5] P. Mathecken, T. Riihonen, S. Werner, and R. Wichman, "Performance analysis of OFDM with Wiener phase noise and frequency selective fading channel," *IEEE Trans. Commun.*, vol. 59, no. 5, pp. 1321–1331, May 2011.

[6] P. Mathecken, N. N. Tchamov, S. Werner, M. Valkama, and R. Wichman, "Characterization of OFDM radio link under PLL-based oscillator phase noise and multipath fading channel," *IEEE Trans. Commun.*, vol. 60, no. 6, pp. 1479–1485, Jun. 2012.

[7] L. Piazzo and P. Mandarini, "Analysis of phase noise effects in OFDM modems," *IEEE Trans. Commun.*, vol. 53, no. 10, pp. 1696–1705, Oct. 2002.

[8] S. Wu and Y. Bar-Ness, "A phase noise suppression algorithm for OFDM-based WLANs," *IEEE Commun. Lett.*, vol. 6, no. 12, pp. 535–537, Dec. 2002.

[9] S. Wu and Y. Bar-Ness, "OFDM systems in the presence of phase noise: consequences and solutions," *IEEE Trans. Commun.*, vol. 52, no. 11, pp. 1988–1996, Nov. 2004.

[10] M.-K. Lee, K. Yang, and K. Cheun, "Iterative receivers based on subblock processing for phase noise compensation in OFDM systems," *IEEE Trans. Commun.*, vol. 59, no. 3, pp. 792–802, Mar. 2011.

[11] D. D. Lin, R. A. Pacheco, T. J. Lim, and D. Hatzinakos, "Joint estimation of channel response, frequency offset, and phase noise in OFDM," *IEEE Trans. Signal Process.*, vol. 54, no. 9, pp. 3542–3554, Sep. 2006.

[12] D. D. Lin, Y. Zhao, and T. J. Lim, "The variational inference approach to joint data detection and phase noise estimation in OFDM," *IEEE Trans. Signal Process.*, vol. 55, no. 5, pp. 1862–1874, May 2007.

[13] Q. Zou, A. Tarighat, and A. H. Sayed, "Compensation of phase noise in OFDM wireless systems," *IEEE Trans. Signal Process.*, vol. 55, no. 11, pp. 5407–5424, Nov. 2007.

[14] P. Rabiei, W. Namgoong, and N. Al-Dhahir, "A non-iterative technique for phase noise ICI mitigation in packet-based OFDM systems," *IEEE Trans. Signal Process.*, vol. 58, no. 11, pp. 5945–5950, Nov. 2010.

[15] N. N. Tchamov, J. Rinne, A. Hazmi, M. Valkama, V. Syrjälä, and M. Renfors, "Enhanced algorithm for digital mitigation of ICI due to phase noise in OFDM receivers," *IEEE Wireless Commun. Lett.*, vol. 2, no. 1, pp. 6–9, Feb. 2013.

[16] V. Syrjälä, M. Valkama, N. N. Tchamov, and J. Rinne, "Phase noise modeling and mitigation techniques in OFDM communications systems," in *Proc. 2009 Wireless Telecommunications Symposium*, pp. 1–7.

[17] F. Septier, Y. Delignon, A. Menhaj-Rivenq, and C. Garnier, "Monte Carlo methods for channel, phase noise, and frequency offset estimation with unknown noise variances in OFDM systems," *IEEE Trans. Signal Process.*, vol. 56, no. 8, pp. 3613–3626, Aug. 2008.

[18] Y.-H. Kim and S.-C. Kim, "Joint channel estimation and phase noise suppression for OFDM systems," *IEICE Trans. Commun.*, vol. E91-B, no. 10, pp. 3371–3374, Oct. 2008.

[19] D. Petrovic, W. Rave, and G. Fettweis, "Effects of phase noise on OFDM systems with and without PLL: characterization and compensation," *IEEE Trans. Commun.*, vol. 55, no. 8, pp. 1607–1616, Aug. 2007.

[20] F. Munier, T. Eriksson, and A. Svensson, "An ICI reduction scheme for OFDM system with phase noise over fading channels," *IEEE Trans. Commun.*, vol. 56, no. 7, pp. 1119–1126, Jul. 2008.

[21] S. Suyama, H. Suzuki, K. Fukawa, and J. Izumi, "Iterative receiver employing phase noise compensation and channel estimation for millimeter-wave OFDM systems," *IEEE J. Sel. Areas in Commun.*, vol. 27, no. 8, pp. 1358–1366, Oct. 2009.

[22] M.-K. Lee, S.-C. Lim, and K. Yang, "Blind compensation for phase noise in OFDM systems over constant modulus modulation," *IEEE Trans. Commun.*, vol. 60, no. 3, pp. 620–625, Mar. 2012.

[23] C. Muschalik, "Improving an OFDM reception using an adaptive Nyquist windowing," *IEEE Trans. Consum. Electron.*, vol. 42, no. 3, pp. 259–269, Aug. 1996.

[24] S. H. Muller-Weinfurtner, "Optimum Nyquist windowing in OFDM receivers," *IEEE Trans. Commun.*, vol. 49, no. 3, pp. 417–420, Mar. 2001.

[25] R. Song and S.-H. Leung, "A novel OFDM receiver with second order polynomial Nyquist window function," *IEEE Commun. Lett.*, vol. 9, no. 5, pp. 391–393, May 2005.

[26] G. E. Bottomley and L. R. Wihelmsson, "Recovering signal energy from the cyclic prefix in OFDM," *IEEE Trans. Vehicular Technol.*, vol. 57, no. 5, pp. 3205–3211, Sep. 2008.

[27] M.-X. Chang, "A novel algorithm of inter-subchannel interference self-cancellation in OFDM systems," *IEEE Trans. Wireless Commun.*, vol. 6, no. 8, pp. 2881–2893, Aug. 2007.

[28] M. Faulkner, L. R. Wilhelmsson, and J. Svensson, "Low-complex ICI cancellation for improving Doppler performance in OFDM systems," in *Proc. 2006 IEEE Vehicular Technol. Conf. – Fall*, pp. 1–5.

[29] C.-R. Sheu, M.-C. Tseng, C.-Y. Chen, and H.-P. Lin, "A low-complexity concatenated ICI cancellation scheme for high-mobility OFDM systems," in *Proc. 2007 IEEE Wireless Commun. and Networking Conf.*, pp. 1389–1393.

[30] C.-R. Sheu, J.-W. Liu, and C.-C. Huang, "A low-complexity ICI cancellation scheme with multi-step windowing and modified SIC for high-mobility OFDM systems," in *Proc. 2010 IEEE Vehicular Technol. Conf. – Spring*, pp. 1–5.

[31] C.-Y. Ma, S.-W. Liu, and C.-C. Huang, "On optimum segment combining weight for ICI self-cancellation in OFDM systems under doubly selective fading channels," in *Proc. 2012 IEEE Vehicular Technol. Conf. – Spring*, pp. 1–5.

[32] K.-Y. Lin, H.-P. Lin, and M.-C. Tseng, "An equivalent channel time variation mitigation scheme for ICI reduction in high-mobility OFDM systems," *IEEE Trans. Broadcast.*, vol. 58, no. 3, pp. 472–479, Sep. 2012.

[33] N. N. Tchamov, V. Syrjälä, J. Rinne, M. Valkama, Y. Zou, and M. Renfors, "System- and circuit-level optimization of PLL designs for DVB-T/H receivers," *Springer J. Analog Integrated Circuits and Signal Process.*, vol. 73, no. 1, pp. 185–200, Oct. 2012.

[34] N. N. Tchamov, A. Hazmi, J. Rinne, M. Valkama, and M. Renfors, "Performance comparison of DVB-T and DVB-T2 in the presence of phase noise," in *Proc. 2010 International OFDM-Workshop*, pp. 1–4.

[35] E. Perahia *et al.*, "TGad evaluation methodology," doc.: IEEE 802.11-09/0296r16, Jan. 2010. Available: http://www.ieee802.org/11/Reports/tgad update.htm.

[36] S. Boyd and L. Vandenberghe, *Convex Optimization*. Cambridge University Press, 2004.

[37] S. Abu-Surra *et al.*, "IEEE P802.11 wireless LANs PHY/MAC complete proposal specification," doc.: IEEE 802.11-10/0433r2. Available: http://www.ieee802.org/11/Reports/tgad update.htm.

[38] A. Maltsev, V. Erceg, E. Perahia, *et al.*, "Channel models for 60GHz wlan systems," doc.:IEEE 802.11-09/0334r8, May 2010. Available: http://www.ieee802.org/11/Reports/tgad update.htm.

**Chun-Ying Ma** was born in 1985, Tainan, Taiwan. He received his B. Eng in communications from National Chiao Tung University, Taiwan, in 2008. He then joined the Wireless Communication Lab of National Chiao Tung University pursuing a Ph.D. degree in the area of wireless communications. His current research interests include high-mobility OFDM communication systems, green radio, wireless resource allocation, and phase noise suppression algorithms.

**Chun-Yen Wu** was born in Taiwan, R.O.C. He received his B.S. degree in Electrical Engineering from Nation Taipei University of Technology in 2010 and M.S. degree in Communications Engineering from National Chiao Tung University in 2012. He is currently a software engineer with MediaTek Corp. in Hsinchu City, Taiwan.

**Chia-Chi Huang** was born in Taiwan, R.O.C. He received the B.S. degree in electrical engineering from National Taiwan University in 1977 and the M.S. and Ph.D. degrees in electrical engineering from the University of California, Berkeley, in 1980 and 1984, respectively. From 1984 to 1988, he was an RF and communication system engineer with the Corporate Research and Development Center, General Electric Company, Schenectady, NY, where he worked on mobile radio communication system design. From 1989 to 1992, he was with the IBM T.J. Watson Research Center, Yorktown Heights, NY, as a Research Staff Member, working on indoor radio communication system design. Since 1992, he has been with National Chiao Tung University, Hsinchu, Taiwan, and currently as a Professor in the Department of Electrical and Computer Engineering.